Direct Detection of Resonant Electron Pitch Angle Scattering by Whistler Waves in a Laboratory Plasma

B. Van Compernolle,[1,*] J. Bortnik,[2] P. Pribyl,[1] W. Gekelman,[1] M. Nakamoto,[1] X. Tao,[2] and R. M. Thorne[2]
[1]Department of Physics, University of California, Los Angeles, California 90095, USA
[2]Department of Atmospheric and Oceanic Sciences, University of California, Los Angeles, California 90095, USA
(Received 9 August 2013; published 10 April 2014)

Resonant interactions between energetic electrons and whistler mode waves are an essential ingredient in the space environment, and in particular in controlling the dynamic variability of Earth's natural radiation belts, which is a topic of extreme interest at the moment. Although the theory describing resonant wave-particle interaction has been present for several decades, it has not been hitherto tested in a controlled laboratory setting. In the present Letter we report on the first laboratory experiment to directly detect resonant pitch angle scattering of energetic (~keV) electrons due to whistler mode waves. We show that the whistler mode wave deflects energetic electrons at precisely the predicted resonant energy, and that varying both the maximum beam energy, and the wave frequency, alters the energetic electron beam very close to the resonant energy.

DOI: 10.1103/PhysRevLett.112.145006 PACS numbers: 94.30.Ny, 52.35.Hr, 52.72.+v, 94.30.Tz

A major scientific problem of current interest is the determination of the dominant physical processes that drive the dynamic variability of the outer radiation belt [1–3]. Over the past decade or so, a number of studies have shown that the traditional view of radiation belt formation, that is, inward radial diffusion balanced by wave-induced scattering [4,5], was insufficient to account for the dramatic, and often unpredictable variability of Earth's outer radiation belt [6,7]. A key component that was missing in previous analyses appears to involve resonant interactions between energetic radiation belt electrons, and natural plasma waves, particularly those waves propagating in the whistler mode (where the wave frequency is between the electron and proton gyro frequencies) [7–11].

The idea of whistler-mode wave-particle interactions is not new by any means, and has appeared in the literature under various contexts such as stochastic scattering and precipitation of energetic electrons into the Earth's dense upper atmosphere [4,12], coherent amplification of injected signals from the transmitter in Siple, Antarctica, and subsequent triggering of secondary emissions [13–15], and most recently, acceleration of seed electrons (~100 keV) to relativistic energies [8,16–18]. In each case, the electron flies through the whistler wave packet and experiences a quasistationary electromagnetic wave field in its frame of reference when its gyro frequency matches the Doppler-shifted frequency of the wave. In this case, the electron and wave are said to be in resonance, and satisfy the equation

$$\omega - kv_{||} = \Omega_e \tag{1}$$

where ω is the wave radial frequency, Ω_e is the electron gyro frequency k is the wave number, assumed to be propagating parallel to the background magnetic field, $v_{||}$ is the electron's velocity component parallel to the background magnetic field, and $kv_{||} < 0$. Studying the interaction between whistler waves and energetic electrons in the laboratory is challenging because of the small scales involved. In a fully magnetized laboratory plasma, i.e., $\rho_i \ll D_{\mathrm{machine}}$, the electron gyro radius is typically mm size or less, making it difficult to detect changes in electron pitch angle. A review of observations and experiments on whistler mode waves is given in [19].

This Letter reports the first direct laboratory detection of the resonant scattering of energetic electrons by whistler mode waves, performed in the Large Plasma Device (LAPD) at UCLA. Energetic electrons emitted from a beam source interact with whistler waves launched by an antenna and propagating counter to the energetic electrons. Signatures of the energetic electrons on a fast particle detector are compared with and without whistler waves present. A resonant interaction is observed when the energetic electrons have the energy needed to Doppler shift the launched whistler mode frequency to the electron cyclotron frequency.

The experiment is performed on the upgraded Large Plasma Device [20,21] at the Basic Plasma Science Facility (BAPSF) at UCLA. The LAPD is a long cylindrical device, with axial magnetic field and a 18 m long 60 cm diameter quiescent plasma column. The plasma is pulsed at 1 Hz, and lasts for 12 ms with several milliseconds of steady state plasma. Plasma parameters for this study were $n_e = 10^{12}$ cm^{-3}, $T_e = 6$ eV, $B_0 = 200$ G with a fill gas of helium. Automated probe drives connected to ball valves [22] enable 3D measurements of plasma parameters.

A 10 cm diameter energetic electron beam source and a whistler wave antenna are introduced into the machine

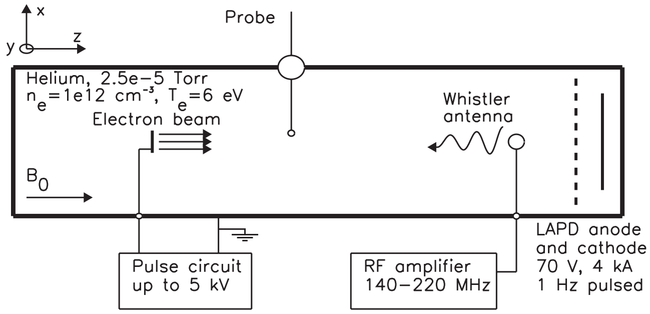

FIG. 1. Sketch of the experimental setup (not to scale). A 10 cm diameter electron beam launches electrons with energies up to 5 keV. Whistler waves are launched on the same field lines with a loop antenna in the frequency range 0.2–0.4 Ω_e. The plasma is diagnosed with Langmuir probes, magnetic field probes and fast particle detectors.

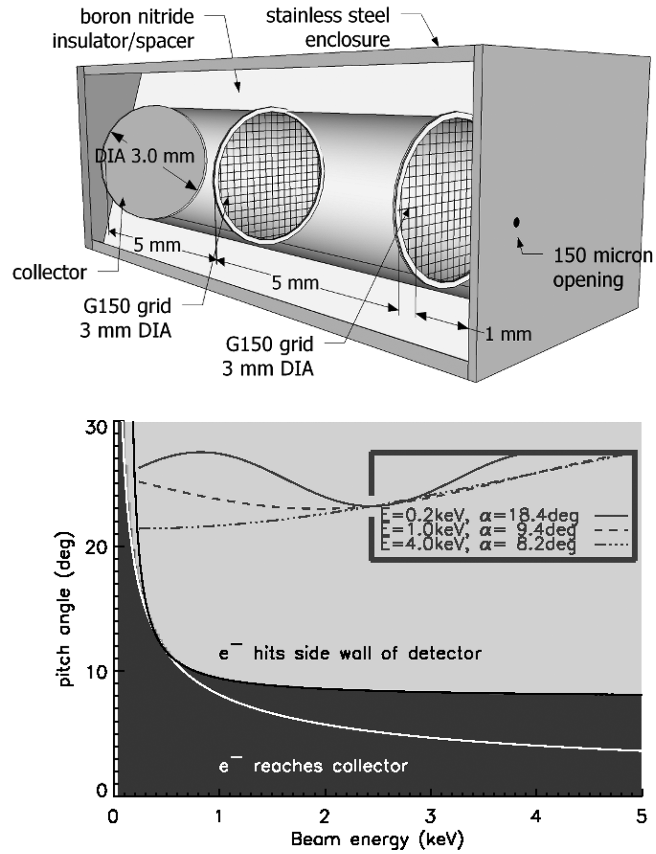

FIG. 2. Upper panel: cutaway view of the fast particle detector, showing the grids, collector, housing and 150 μm entrance hole. Lower panel: Calculated pitch angle sensitivity of the fast particle detector as a function of electron beam energy. Electrons with $E > 0.5$ keV and pitch angle larger than 10° will hit the side wall and will not be detected.

(Fig. 1). Measurements are taken in the region between the whistler wave antenna and the electron beam source. The electron beam source is based on a lanthanum hexaboride cathode (LaB_6) developed earlier at LAPD [23], with a series of grids separated by ceramic insulating spacers on the front side. The 10 cm diameter LaB_6 disk is heated to emission temperatures ($T > 1500\,°C$) and pulsed negatively with respect to the machine wall ($0.5 \le V_{beam} \le 3$ kV). The start of the electron beam pulse is taken as $t = 0$ and the location of the electron beam source as $z = 0$. The whistler wave antenna is inserted in the machine a distance 6.4 m away from the electron beam source. The antenna consists of a balanced loop, 1 cm in diameter and oriented with its normal perpendicular to the magnetic field. The antenna is powered by a 2 kW radio frequency amplifier, which is broadband up to 220 MHz. Whistler wave frequencies are in the range of 0.2–0.4 Ω_e, representative of natural magnetospheric chorus waves in space [1,14]. For these parameters the beam electron energy needed for resonance varies from 0.5 up to a few keV.

The fast electrons are diagnosed with a fast particle detector (Fig. 2). It consists of two 3 mm diameter grids and a collector held in place by cylindrical insulating boron nitride spacers and housed in a stainless steel enclosure. At the front of the detector a 150 μm entrance hole limits the particle flux and density in the detector. The grids are biased in order to screen out the Maxwellian plasma population. Both the electron beam source and the detector are aligned along the magnetic field, i.e., the normal to the grids is parallel to the background field. In the limit of zero pitch angle, electrons entering the detector with energy above 75 eV reach the collector. It is clear however that electrons with nonzero pitch angle could have a large enough gyro radius such that they hit the side of the detector and never reach the collector. Figure 2 shows the threshold pitch angle at different electron beam energies for this to happen. In the low energy range the limiting factor for an electron to hit the side wall is set by the gyro radius and the radius a of the detector, i.e., $(v_\perp/\Omega_e) > (a/2)$. At higher energies the parallel velocity of the electron can be large enough such that the electron reaches the collector before hitting the side wall, even though the gyro radius satisfies the previous condition. The necessary condition for hitting the side wall of the detector then becomes $(v_\perp/\Omega_e)\sin(\Omega_e L/2v_\parallel) > (a/2)$, where L is the length of the detector. These two conditions are plotted as the white and black curves respectively in Fig. 2. Example trajectories of electrons hitting the side walls are plotted in the inset. Figure 2 shows that for our conditions ($B_0 = 200$ G, $a = 1.5$ and $L = 11$ mm) electrons will not reach the collector if their pitch angle is larger than roughly 10 degrees in the energy range of 0.5 to 5 keV. Signals on the fast particle detector in the presence of whistler waves are compared to the signals without whistler waves. A decrease in the signal strength will be attributed to scattering of electrons to higher pitch angles, i.e., into the loss cone of the detector.

The perpendicular spatial profiles of the electron beam current density and whistler waves are displayed in Fig. 3.

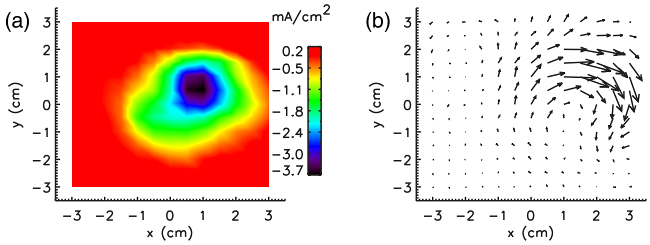

FIG. 3 (color online). Profiles of electron beam current density, panel (a), and whistler wave magnetic field, panel (b), in a plane perpendicular to the background field. Beam densities are on the order of 10^{-5} of the plasma density and whistler amplitudes are on the order of 10^{-4} the background magnetic field.

Panel (a) shows the electron beam current density, measured with the fast particle detector. It is close to a Gaussian profile slightly distorted due to the plasma density reduction in the shadow of the whistler wave antenna. The profile was measured for a 2 kV accelerating potential on the beam source. Signals on the probe are in the range of 4 mA/cm^2 which for 2 keV electrons translates into beam densities of 10^7 cm^{-3}, equivalent to $n_{\text{beam}}/n_e \simeq 10^{-5}$. The beam density is kept low in order to limit the beam generated whistler waves to a level much lower than the whistler waves launched by the antenna.

The perpendicular magnetic field for a 180 MHz whistler wave is plotted as a vector plot in Fig. 3(b). The spatial extent of the whistler wave is similar to that of the electron beam. Care was taken in the experiment to ensure both profiles overlap. Time traces show that the B_y component lags the B_x component by 90°; i.e., the measured wave is right handed as expected for the whistler wave. The magnetic fields in panel (b) are on the order of 2 mG, but in the experiment the whistler wave antenna is typically operated at higher powers resulting in fields up to 30 mG, i.e., $B_{\text{wave}}/B_0 \simeq 10^{-4}$.

Figure 4(a) shows time traces of the beam voltage, and the current density to the fast particle detector both with and without whistler waves. The voltage on the beam source is not fixed, but is instead ramped up in 40 μs to a predetermined maximum beam voltage and then ramped down in about 400 μs. In one plasma shot beam electrons having energies from several keV to less than 100 eV are launched. This approach was favored over operating with a fixed beam energy since the interaction of whistler waves with beam electrons can be studied for a range of beam energies in one plasma shot. The transit time of a beam electron through the machine ($\simeq$1 μs) is much less than the 400 μs over which the beam is ramped down. The ramp down of the beam voltage is therefore slow enough to have good resolution in beam energies.

The whistler waves, if present, are on for the time displayed in Fig. 4(a) and are launched with a frequency of 180 MHz. Both time traces on the fast particle detector overlap for some of the time, but a decrease in signal

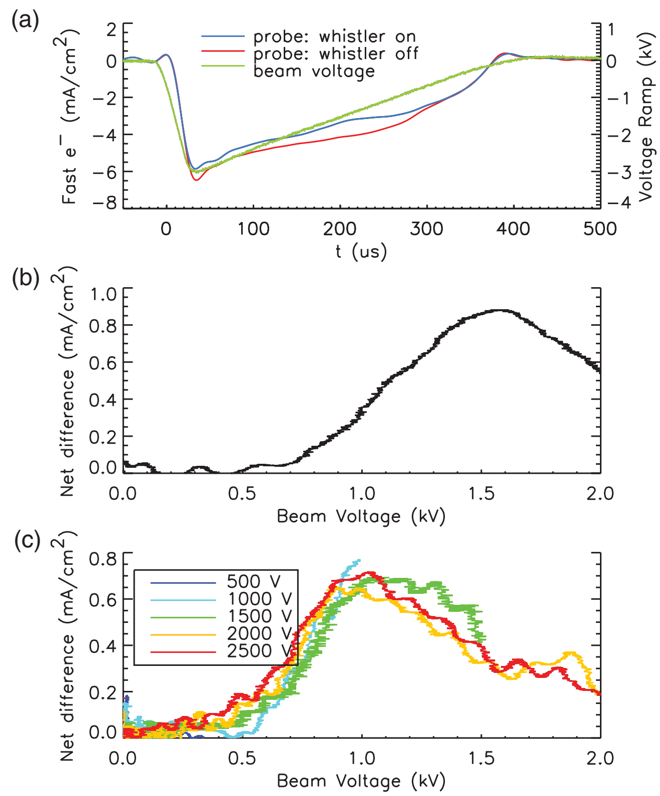

FIG. 4 (color). Panel (a): time traces of beam voltage and measured electron beam current density both with and without the whistler wave present where $f = 180$ MHz. Panel (b): difference of beam current density with/without whistler waves plotted versus beam voltage with $f = 180$ MHz. Panel (c): difference signal with maximum beam ramp voltage ranging from 0.5 to 2.5 kV and $f = 200$ MHz.

strength is seen for a certain range of electron beam energies. Panel (b) shows the difference between the detector signals with and without whistler waves, plotted versus beam voltage. There is a threshold beam voltage of 0.8 kV below which no scattering is observed. The velocity of the energetic electrons is below the resonant velocity and equation (1) cannot be satisfied. Resonance only occurs once the beam voltage reaches or exceeds the resonant energy. A theoretical estimation of the resonant electron beam energy in the case of 180 MHz whistler waves at a background field of 200 G yields 0.84 keV as the resonant electron beam energy, assuming $k_\perp = 0$. Relaxing this to arbitrary $k_\perp$ yields a range of resonant electron beam energies. Note that there is still substantial interaction at higher energies. This is due to the initial beam being unstable to waves and therefore becoming a Maxwellian with a long high energy tail with energies up to the applied beam voltage away from the beam source [24,25]. In other words, an electron beam launched with 3 kV on the beam source will have fast electrons of lower energies due to beam thermalization. The lower energy electrons at $E \simeq$ 0.8 keV can then undergo a resonant interaction with the

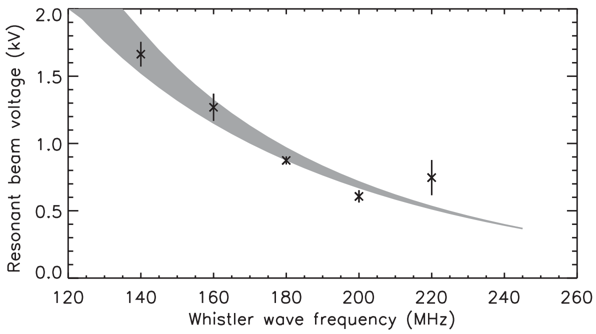

FIG. 5. Threshold beam voltage, i.e., resonant electron energy, for signal reduction on the fast particle detector. Shaded region represents the theoretical prediction for $n = 1.1 \times 10^{12}$ cm^{-3}, for a range of $k_\perp$ from 0 cm^{-1} up to 1 cm^{-1}, obtained from the data in Fig. 3(b). $k_\parallel$ at 180 MHz ranges from 1.36 to 1.29 cm^{-1} inferred from the whistler dispersion relation.

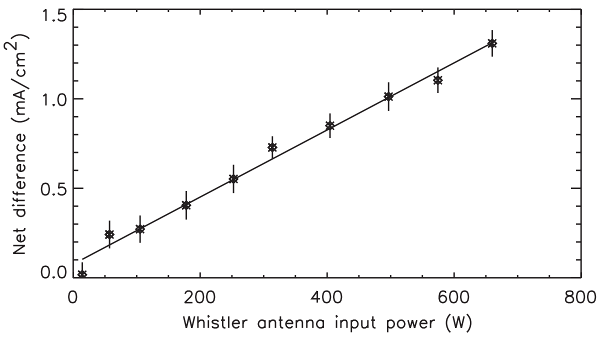

FIG. 6. Signal reduction on fast particle detector versus whistler wave input power, taken at $x = 1.5$ cm, $y = 0.5$ cm.

whistler waves and a change in fast detector signal will be observed, even for 3 kV on the beam source. For this reason the threshold beam voltage above which scattering is observed will be taken to correspond to the resonant energy.

In order to solidify the finding that the observed scattering is a real effect, the predetermined maximum voltage on the beam was changed from 0.5 to 2.5 kV. The resonant energy is the same for all cases but will occur at different times in the beam voltage ramp. The signal reduction when the whistler waves are on as in Fig. 4(a) should therefore shift accordingly in time. This was indeed observed and the detected difference in beam density between whistlers on or off plotted versus beam voltage as in Fig. 4(c) showed excellent overlap for all cases. Note that the resonant energy in Fig. 4(c) is downshifted compared to Fig. 4(b) because of the higher whistler wave frequency.

The dependence of the electron beam–whistler wave interaction on the frequency of the whistler wave is shown in Fig. 5. The frequency of the whistler waves was incremented in 20 MHz steps from 140 to 220 MHz. The voltage ramp on the beam was kept fixed with the beam voltage peaking at 3 kV. Figure 5 shows the threshold beam voltage, i.e., resonant energy, for signal reduction on the fast particle detector due to the presence of whistler waves as a function of whistler wave frequency. It shows that decreasing the whistler wave frequency drives the resonant electron energies to higher values. A quantitative comparison to the resonance condition can be made from Fig. 5. The shaded region represents the resonance condition $\omega - \mathbf{k} \cdot \mathbf{v} = \Omega_e$, for the range of $k_\perp$ values present in the experiment [Fig. 3(b)]. Very good agreement is obtained. Figure 5 shows qualitatively and quantitatively that a resonant interaction is occurring at the electron cyclotron frequency in the moving frame of the fast electrons.

The dependence on whistler wave power was investigated to help understand the scattering mechanism. The energy density in the whistler wave in the plasma was found to scale linearly with input power, with magnetic field amplitudes in the range of 30 mG ($\delta B/B_0 \simeq 10^{-4}$). The whistler wave was launched at 180 MHz. Figure 6 shows the maximum signal reduction for each whistler wave power. The signal reduction is found to be approximately linearly proportional to the whistler wave input power, which could be an early indication that the nature of the wave-particle interaction is quasilinear.

In summary, we have shown results from the first experiment to measure the pitch angle scattering of energetic electrons due to resonant wave-particle interactions with whistler mode waves in a laboratory plasma. We have demonstrated that there is a distinct and measurable difference in the intensity of the received energetic electron beam for times when the whistler wave is switched on, compared to when it is off. Moreover, this difference in beam intensities appears at the exact time when the beam energy matches the resonant energy of the electrons. Keeping the beam voltage (i.e., fast particle energy) constant, we varied the whistler wave frequency and showed that the difference in the signal when the whistler was on versus off followed the resonant behavior very closely.

Resonant interactions between energetic electrons and whistler mode waves are an essential ingredient in the space environment, and in particular in controlling the dynamic variability of the Earth's natural radiation belts, which is a currently topic of extreme interest [2]. By devising a laboratory experiment that can reproduce such resonant interactions, we have created a tool that is able to test and evolve wave-particle interaction theories that have been standard in the literature for decades and extensively relied upon for modeling radiation belt behavior, but that have not as-yet been effectively tested under controlled conditions.

The research was funded by the Department of Energy and the National Science Foundation by NSF Grant No. 0903802 and DE-SC0010578, which was awarded to UCLA through the NSF/DOE Plasma Partnership program. Work was done at the Basic Plasma Science Facility (BAPSF) also funded by DOE/NSF.

*bvcomper@physics.ucla.edu

[1] R. M. Thorne, Geophys. Res. Lett. **37**, L22107 (2010).
[2] B. H. Mauk, in *Dynamics of the Earth's Radiation Belts and Inner Magnetosphere* (American Geophysical Union, Washington, DC, 2012), p. 405.
[3] G. D. Reeves, H. E. Spence, M. G. Henderson, S. K. Morley, R. H. W. Friedel, H. O. Funsten, D. N. Baker, S. G. Kanekal, J. B. Blake, J. F. Fennel, S. G. Claudepierre, R. M. Thorne, D. L. Turner, C. A. Kletzing, W. S. Kurth, B. A. Larsen, and J. T. Niehof, Science **341**, 991 (2013).
[4] L. R. Lyons and R. M. Thorne, J. Geophys. Res. **78**, 2142 (1973).
[5] M. Schulz and L. J. Lanzerotti, *Particle Diffusion in the Radiation Belts* (Springer-Verlag, Berlin, 1974).
[6] G. D. Reeves, K. L. McAdams, R. H. W. Friedel, and T. P. O'Brien, Geophys. Res. Lett. **30**, 36 (2003).
[7] R. B. Horne, R. M. Thorne, S. A. Glauert, J. M. Albert, N. P. Meredith, and R. R. Anderson, J. Geophys. Res. **110**, A03225 (2005).
[8] R. B. Horne and R. M. Thorne, Geophys. Res. Lett. **30**, 1527 (2003).
[9] J. M. Albert, N. P. Meredith, and R. B. Horne, J. Geophys. Res. **114**, A09214 (2009).
[10] A. Varotsou, D. Boscher, S. Bourdarie, R. B. Horne, N. P. Meredith, S. A. Glauert, and R. H. Friedel, J. Geophys. Res. **113**, A12212 (2008).
[11] Y. Y. Shprits, D. Subbotin, and B. Ni, J. Geophys. Res. **114**, A11209 (2009).
[12] C. F. Kennel and H. E. Petschek, J. Geophys. Res. **71**, 1 (1966).
[13] R. A. Helliwell, *Whistlers and Related Ionospheric Phenomena* (Stanford University Press, Stanford, CA, 1965).
[14] R. A. Helliwell and T. L. Crystal, J. Geophys. Res. **78**, 7357 (1973).
[15] K. B. Dysthe, J. Geophys. Res. **76**, 6915 (1971).
[16] D. Summers, R. M. Thorne, and F. Xiao, J. Geophys. Res. **103**, 20487 (1998).
[17] J. Bortnik, R. M. Thorne, and U. S. Inan, Geophys. Res. Lett. **35**, L21102 (2008).
[18] J. M. Albert, X. Tao, and J. Bortnik, in *Dynamics of the Earth's Radiation Belts and Inner Magnetosphere* (American Geophysical Union, Washington, DC, 2012), p. 255.
[19] R. L. Stenzel, J. Geophys. Res. **104**, 14379 (1999).
[20] W. Gekelman, H. Pfister, Z. Lucky, J. Bamber, D. Leneman, and J. Maggs, Rev. Sci. Instrum. **62**, 2875 (1991).
[21] D. Leneman, W. Gekelman, and J. Maggs, Rev. Sci. Instrum. **77**, 015108 (2006).
[22] D. Leneman and W. Gekelman, Rev. Sci. Instrum. **72**, 3473 (2001).
[23] B. Van Compernolle, W. Gekelman, P. Pribyl, and C. Cooper, Phys. Plasmas **18**, 123501 (2011).
[24] A. A. Ivanov and L. I. Rudakov, Sov. Phys. JETP **24**, 1027 (1967).
[25] S. Kainer, J. Dawson, R. Shanny, and T. Coffey, Phys. Fluids **15**, 493 (1972).